Review

Paul Linsdell*

Metal bridges to probe membrane ion channel structure and function

DOI 10.1515/bmc-2015-0013
Received April 27, 2015; accepted May 29, 2015

Abstract: Ion channels are integral membrane proteins that undergo important conformational changes as they open and close to control transmembrane flux of different ions. The molecular underpinnings of these dynamic conformational rearrangements are difficult to ascertain using current structural methods. Several functional approaches have been used to understand two- and three-dimensional dynamic structures of ion channels, based on the reactivity of the cysteine side-chain. Two-dimensional structural rearrangements, such as changes in the accessibility of different parts of the channel protein to the bulk solution on either side of the membrane, are used to define movements within the permeation pathway, such as those that open and close ion channel gates. Three-dimensional rearrangements – in which two different parts of the channel protein change their proximity during conformational changes – are probed by cross-linking or bridging together two cysteine side-chains. Particularly useful in this regard are so-called metal bridges formed when two or more cysteine side-chains form a high-affinity binding site for metal ions such as Cd^{2+} or Zn^{2+}. This review describes the use of these different techniques for the study of ion channel dynamic structure and function, including a comprehensive review of the different kinds of conformational rearrangements that have been studied in different channel types *via* the identification of intra-molecular metal bridges. Factors that influence the affinities and conformational sensitivities of these metal bridges, as well as the kinds of structural inferences that can be drawn from these studies, are also discussed.

Keywords: cysteine; disulfide; ion channel; metal bridge; substituted cysteine accessibility mutagenesis.

***Corresponding author: Prof. Paul Linsdell,** Department of Physiology and Biophysics, Dalhousie University, PO Box 15000, Halifax, Nova Scotia B3H 4R2, Canada, e-mail: paul.linsdell@dal.ca

Introduction

Membrane proteins, including receptors, transporters, pumps, and ion channels, are involved in almost all aspects of communication between individual cells and their environment. However, because these proteins exist embedded in the lipid membrane, their structure is difficult to study directly using techniques such as crystallography. Furthermore, membrane proteins have to undergo substantial conformational changes as they transmit signals between the extracellular environment and the interior of the cell, and the nature and extent of these dynamic conformational changes are not apparent from static structural images. For these reasons, a wealth of alternative approaches have been developed to study the dynamic aspects of the structure and function of membrane proteins in their native, membrane-embedded environment, using functional readouts that are sensitive to changes in protein conformation. Several of these approaches take advantage of the unique chemistry of the cysteine side-chain among the natural amino acids that make up proteins. The cysteine side-chain contains a thiol group (-SH) that can be readily deprotonated to form a reactive thiolate anion ($-S^-$) that is capable of nucleophilic attack on electrophilic centers. Under oxidizing conditions, this leads to the rapid formation of disulfide bonds with other nearby sulfur-containing groups. In native proteins this process leads to the redox-sensitive formation of inter- or intra-molecular disulfide bonds between pairs of cysteine side-chains (1, 2). It can also be used to label covalently cysteine side-chains in proteins *in situ* with designer probes containing reactive sulfur groups such as thiosulfonates. Polarizable, anionic cysteine thiols also bind a number of metal ions, such as Cu^{2+}, Zn^{2+}, Cd^{2+}, Hg^+, and Ag^+ (3–7). Coordination of the metal ligand resulting from simultaneous interaction with multiple cysteine side-chains results in increased affinity metal binding, effectively forming a high-affinity metal 'bridge' between two or more (potentially up to four) cysteine side-chains (3–5).

Cysteine-specific probes are used in combination with site-directed mutagenesis to introduce a cysteine

side-chain into any part of a protein. At the two-dimensional level, reactivity of the cysteine side-chain can then be used to identify the location of amino acids in any part of the primary sequence, their relative accessibility from different sides of the membrane, and changes in accessibility during protein conformational changes. At the three-dimensional level, the proximity of different amino acids can be ascertained using substances that can generate cross-links or bridges between two cysteine side-chains introduced into two different parts of the protein. Again, changes in amino acid proximity during conformational changes in the protein can give valuable insights into the nature and extent of the protein movements that are involved in these conformational changes. These techniques have been used most extensively to study the structure and function of ion channels, the function of which is relatively accessible using electrophysiological techniques to measure the tiny current that flows across the membrane carried by these channel proteins; the current review is focused on these channel proteins. However, in principle these techniques can be used to study any membrane protein for which some aspect of structure or function can be monitored experimentally (8–17).

Two-dimensional information: substituted cysteine accessibility mutagenesis

The technique of substituted cysteine accessibility mutagenesis (SCAM) was first developed to study the structure of ion channels (18, 19) and has since been applied to almost all channel types as well as many other classes of proteins. This technique is based on the covalent reaction between the cysteine thiol and the thiosulfonate group of small, hydrophilic molecules, and rests on the assumption that this covalent modification will lead to some change in protein function that can be easily monitored. The most commonly used probes are small methanethiosulfonate (MTS) reagents such as the negatively charged [2-sulfonatoethyl] methanethiosulfonate (MTSES), the positively charged [2-(trimethylammonium)ethyl] methanethiosulfonate (MTSET), and the neutral/partially positively charged [2-aminoethyl] methanethiosulfonate (MTSEA) (20). Because these thiosulfonates are highly hydrophilic, and also because they react at least 5×10^9 times faster with the ionized ($-S^-$) form of the cysteine thiolate than the uncharged (-SH) form, it is assumed that any reaction will be with cysteine side-chains that are on a water-accessible surface of the protein. When the reaction is with a cysteine in the membrane-spanning part of a transmembrane protein such as an ion channel, it is most likely that this water-accessible surface is the lining of the permeation pathway or some other water-filled crevice in the protein (Figure 1B). Cysteine side-chains can be introduced into any part of the channel protein using site-directed mutagenesis. In this way, channel pore-lining residues can be identified by sequentially 'scanning' membrane-spanning parts of the protein, which is to say that each amino acid is mutated, one at a time, to cysteine, and its accessibility to MTS reagents tested using functional approaches. Assuming that covalent modification of a pore-lining cysteine side-chains by a small charged reagent will alter channel function in some way, electrophysiological techniques can then be used to discriminate pore-lining (reactive) from non-pore-lining (non-reactive) cysteine side-chains, with the caveat that a negative result could reflect either non-reactivity or reactivity that is without measureable functional consequence. MTS reagents react rapidly with the cysteine thiol; the rate of reaction between these reagents and the thiol of β-mercaptoethanol (β-ME) in free solution is $>10\,000\ M^{-1}\ s^{-1}$ (20). However, the measured reaction rate with cysteine side-chains in ion channels may be considerably less due to restricted access from the bulk solution to the channel pore. Furthermore, where the introduced cysteine is in a part of the protein that undergoes significant conformational changes, the rate of modification may be different in different conformations (Figure 1A,B). Because MTS reagents form a stable disulfide bond with the cysteine thiol, the functional effects of MTS reagents are expected to be sustained even after these reagents have been washed from the experimental chamber; however, they can usually be reversed using reducing agents such as dithiothreitol (DTT) or β-ME to break the disulfide bond. To avoid the possibility of reaction with native cysteines, SCAM studies should be carried out using functional versions of proteins in which all endogenous cysteine residues have been replaced by other amino acids using site-directed mutagenesis (so-called cys-less protein backgrounds). However, in practice, many published ion channel SCAM studies use wild-type backgrounds including some or all native cysteines, so long as the wild-type background is found to be non-responsive to application of MTS reagents. Use of a cys-less protein background simplifies interpretation of the experimental results, since an introduced cysteine is the only possible target of cysteine-reactive reagents, but it also has its own potential pitfalls. Most importantly, removal of endogenous cysteines can impact the function of the protein. For example, in the

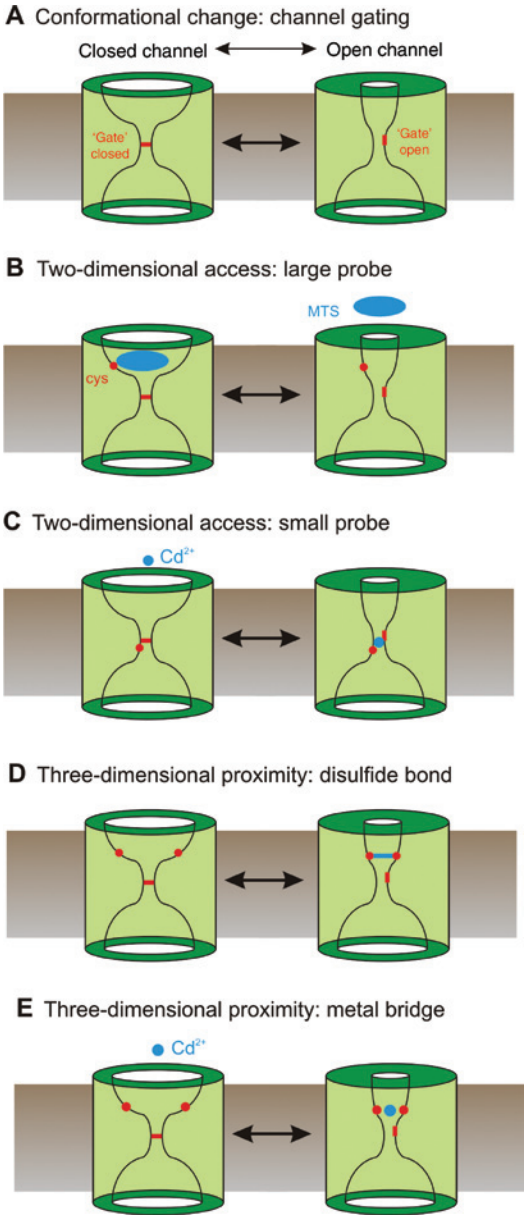

Figure 1: Conceptual overview of the ways in which cysteine chemistry is used to probe conformational changes in ion channel proteins. As an example, this overview considers a conformational change that opens and closes the channel pore. (A) Channel opening is controlled by a localized 'gate', in this example located in the narrow central region of the pore; although it is noted that in some channel types, the gate is not located in the narrow region. (B) Large probes such as MTS reagents may access wide, outer parts of the pore in one conformation only (in this case, in the closed state) to react covalently with an introduced cysteine side-chain (cys). (C) Smaller probes such as Cd^{2+} are expected to have access to all parts of the pore and therefore should report conformational changes that are relevant to the permeant ion (in this case, opening of the channel gate). (D) Two cysteine side-chains are close enough together to form a disulfide bond (blue line) only in the open state, effectively 'locking' the channel in this state. (E) Two cysteine side-chains are close enough together to form a metal bridge only in the open state, effectively stabilizing the channel in this state in the presence of Cd^{2+} ions.

cystic fibrosis transmembrane conductance regulator (CFTR) Cl^- channel, removal of the 18 endogenous cysteine residues to create a cys-less protein severely compromises protein trafficking to the cell membrane (21), necessitating maneuvers such as additional mutations and growing transfected cells at reduced temperature (~27°C) for functional studies on cys-less CFTR expressed in mammalian cells (22). Cys-less CFTR also has a slightly (15%–20%) elevated single-channel conductance, which was shown to be due to substitution of a single cysteine residue (C343) in a membrane-spanning part of the protein (23). Furthermore, introducing cysteines into different parts of the protein can also alter channel function, although such functional changes are often ignored if they do not prevent SCAM investigation. Again taking CFTR as an example, individual cysteine residues introduced into a cys-less background have been shown to cause complete protein mis-trafficking (even in cells grown in culture at 27°C) (24), to drastically reduce single-channel conductance (25, 26), and to modify channel gating (24). Other practical aspects of SCAM for the study of ion channels and other proteins have been described in detail previously (8–12, 20).

MTS reagents are excellent probes for cysteines located on the surface of proteins, including relatively accessible regions close to the wide entrances to aqueous ion channel pores (Figure 1B). However, channel pores usually narrow to a region that is not much wider than the permeant ion (usually a few angstroms), and these narrow regions may be inaccessible to large MTS reagents (Figure 1B): for example, MTSES, MTSET, and MTSEA fit into a cylinder approximately 6 Å in diameter and 10 Å in length (20). Indeed, MTS reagents are usually considered to be impermeant in ion channel pores, implying that there are parts of the permeation pathway that cannot be accessed by these reagents. For these reasons, smaller probes have also been used extensively to test the accessibility of cysteine side-chains introduced into ion channel pores. Small transition metal ions also bind to cysteine side-chains, albeit reversibly, a fact that is reflected in nature in the use of cysteine side-chains in the binding sites for metals such as Cu^{2+}, Zn^{2+}, and Cd^{2+} in many metalloproteins (3–5, 27). The ionic radii of some of these metal ions (e.g. Cd^{2+}, 1.09 Å; Zn^{2+}, 0.88 Å; Ag^+, 1.29 Å) are similar to those of biologically relevant ion channel cationic substrates (K^+, 1.52 Å; Na^+, 1.16 Å; Ca^{2+}, 1.14 Å) (28). As such, these thiophilic metal ions are expected to have access to all parts of ion channel pores that are visited by the natural permeant ion (Figure 1C), and Cd^{2+}, Zn^{2+}, and Ag^+ have all been used as probes of cysteine side-chains introduced into different cation channel pores (29–32).

One major difference between the use of metal ions and MTS reagents is that the interaction between metal ions and cysteine side-chains is expected to be reversible, and so the functional effects of metal ions should be reversed once these ions have been washed from the experimental chamber.

Because the dimensions of these thiophilic metal ion probes closely match those of the natural substrate, it is to be expected that they will be subject to similar restrictions on accessibility to different parts of the pore as the channel transitions between different open and closed conformational states (Figure 1C). As a result, these small probes have been used successfully to identify the location of ion channel 'gates' that open and close to allow or prevent the flow of ionic current and so control the overall function of K^+ channels (33–36), hyperpolarization-activated (HCN) channels (37), cyclic nucleotide-gated channels (38), TRPV1 channels (39), and purinergic P2X receptor channels (40, 41). State-dependent interactions of metal ions with introduced cysteines may also probe other conformational changes occurring within ion channel pores, such as those that control channel inactivation (42–45).

Thiophilic metal ions such as Cd^{2+} have also been used to identify accessible cysteine side-chains introduced into narrow regions of anion-selective channel pores (46). In these channels, however, cationic metal ions cannot be described as appropriate substitutes for the normal anionic permeant anions such as Cl^- and HCO_3^-. Small anions $Au(CN)_2^-$ and $Ag(CN)_2^-$ have been shown to interact covalently with cysteine side-chains introduced into the pore of the CFTR Cl^- channel by a process of ligand exchange (47, 48). Because these small monovalent anions are highly permeant in CFTR (49, 50), they have been used to probe cysteines introduced throughout the pore region (48, 51–55). These small anions have also been used to probe the location of the channel 'gate' that opens and closes the CFTR Cl^- channel (53, 55, 56) as well as other conformational changes in the CFTR pore (51, 54). Because these reactive anions are able to make a covalent reaction with cysteine side-chains, their effects should be irreversible on washing; however, the covalent reaction can be reversed using DTT or excess CN^- (47).

Three-dimensional information: cysteine cross-linking

The reactivity of the cysteine thiol group allows individual cysteine side-chains to make covalent attachments to other, nearby cysteine side-chains *via* reversible disulfide bond formation (1, 2). Because disulfide bond formation and breakage is highly sensitive to redox conditions, reversible disulfide bond formation is used in nature to produce oxidant-sensing proteins (2). Again, researchers have taken extensive advantage of the natural process of cysteine-cysteine disulfide bond formation to investigate the structure and function of membrane proteins. Pairs of cysteine side-chains introduced into different regions of channel proteins using site-directed mutagenesis can be induced to form disulfide bonds under oxidizing conditions provided that the two cysteine side-chains are in close proximity, potentially providing a great deal of three-dimensional information on protein structure and dynamics.

In practical terms, the use of disulfide chemistry to probe membrane proteins involves introduction of two cysteines into different parts of the protein that are hypothesized to be located close together in three-dimensional space, at least at some point in the range of conformational states in which the protein can exist. The formation and breakage of disulfide bonds between the two cysteine side-chains can then be ascertained by some change in protein function (for example, a change in ion channel activity monitored using electrophysiological recording techniques) (57–60), or some other parameter, such as a change in protein mobility on SDS-PAGE gels (11). Because of the potential to form disulfide bonds between an introduced cysteine and any native cysteine side-chains that may exist in the protein under investigation, it is highly desirable to carry out such experiments using cys-less versions of the protein (see above).

In the simplest case, disulfide bonds might form spontaneously between two introduced cysteine side-chains. In this case, channel function may be altered upon exposure to a reducing agent (usually DTT) to break the disulfide bond. However, in mammalian cells, this spontaneous disulfide formation usually only applies to external cysteines, due to the reducing conditions of the cytoplasm. In most cases, an oxidizing agent is applied to induce disulfide bond formation (preferably after treatment with DTT to reduce any disulfide bonds that might have formed spontaneously). A common choice for cysteine side-chains that are exposed on the surface of the protein is copper(II)-*o*-phenanthroline (CuPhe) (61), which catalyzes oxidation by ambient molecular oxygen to promote effective disulfide bond formation, although other strong oxidizing agents such as H_2O_2 or I_2 may also be effective.

The ability of two identified cysteine side-chains to form a disulfide bond is used to provide evidence for the proximity of those side-chains in the three-dimensional

structure of the protein. For a disulfide bond to form, it is thought that the S-S distance must be ~2 Å, with the Cβ-Cβ distance ~3.5–4.6 Å and the Cα-Cα distance ~3.8–6.8 Å, along with strict limits on each of the dihedral angles Cα-Cβ, Cβ-S, and S-S (62–66) (Figure 2). However, it has been found that cysteine side-chains with Cα-Cα distances >15 Å in the equilibrium structure can form disulfide bonds, which is presumed to reflect the effects of protein thermal fluctuations (11, 63).

More distant cysteine side-chains can be connected experimentally using chemical cross-linkers that contain two cysteine-reactive groups. For example, homobifunctional cross-linkers containing two thiol-reactive MTS groups connected by spacer arms of different lengths have been used as 'molecular rulers' to gauge the distances between pairs of cysteine residues introduced into membrane proteins including P-glycoprotein (67), CFTR Cl^- channel (68, 69), lactose permease (70), cyclic nucleotide gated channels (71), KCNQ1/KCNE1 voltage-gated K^+ channels (72), and ENaC Na^+ channels (73). One caveat to the use of these reagents is that long spacer arms result in considerable flexibility of the cross-linker molecule (70), such that cysteine-cysteine distances judged using these cross-linkers should be considered maximal distances and may in fact be considerably less.

Conformational movements are necessary for many aspects of membrane protein function, and disulfide bond formation can be used to obtain important information on the relative proximity of different parts of the protein in different conformational states that may not be accessible using other techniques (Figure 1D). The principle here is that, if the physical proximity of two reporter cysteine side-chains changes concomitant with a conformational change, then (i) disulfide bond formation may be possible only in the conformation in which the two side-chains are close together and/or (ii) disulfide bond formation may 'trap' or 'lock' the protein in the native conformation in which the two cysteine side-chains are close together [and conversely, disulfide bond breakage using DTT will liberate the protein to transition into other conformation(s)]. As shown by the selected examples listed in Table 1, the use of engineered disulfide bond formation has shed light on many different kinds of conformational changes that are crucial to the normal activity of many different classes of ion channels.

Three-dimensional information: cysteine-metal bridging

Cysteine cross-linking has provided a great deal of information on the three-dimensional structure of ion channel proteins and on the three-dimensional nature of conformational changes in these proteins (Table 1). However, the essentially irreversible nature of the disulfide bond under non-reducing conditions limits the information that can be obtained in this way. As described above, whereas the formation of the disulfide bond is subject to strict spatial constraints, it has been observed that relatively distant cysteine side-chains can form disulfide bonds under rare conditions due to protein flexibility. This potential caveat is particularly acute when the aim is to study protein conformational changes. The overall rate at which disulfide bonds will form is dependent on both the relative occupancy of different protein conformations and the proximity of cysteine side-chains in these different conformations. Thus, if disulfide bonds form rapidly in an uncommon (or even unnatural) conformation, cross-linked proteins will tend to accumulate in that conformation due to the high strength of the disulfide bond (often referred to as 'disulfide trapping').

An alternative approach is to use the propensity of cysteine (or other) side-chains to coordinate the binding of metal ions (so-called metal bridge formation). Two or more cysteine side-chains in close proximity can tightly bind metal ions such as Cd^{2+} or Zn^{2+}, resulting in a metal bridge that stabilizes the protein in the conformation in

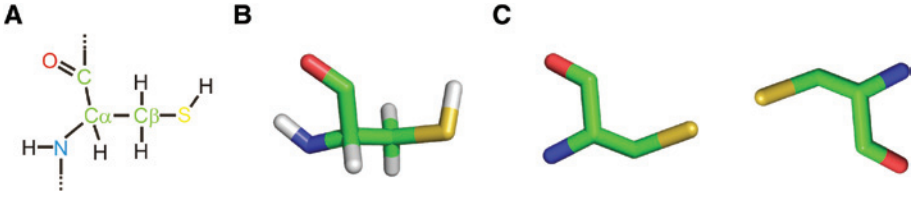

Figure 2: Structure of the cysteine side-chain and experimentally derived proximity of cysteine pairs.
(A) Chemical composition of the cysteine side-chain within a peptide chain. (B) Stick model of the cysteine side-chain. (C) As described in the text, to form either disulfide bonds or metal bridges, the two cysteine side-chains are subject to strict spatial constraints (S-S, Cβ-Cβ, Cα-Cα), as well as limited regarding the dihedral angles Cα-Cβ, Cβ-S, and S-S.

Table 1: Examples of conformational changes in ion channels probed by formation of engineered disulfide bonds.

Channel type	Region of channel protein	Conformational information obtained	References
Voltage-gated channel superfamily			
Shaker K^+ channel	Extracellular ends of transmembrane (TM) segments	Relative movement of different TMs is required for channel opening	(77)
Ca^{2+}-activated K^+ channel	Extracellular ends of TMs	Extracellular ends of TMs move in concert during channel opening	(94)
Ca^{2+}-activated K^+ channel	Extracellular ends of TMs in α and β subunits	Channel opening involves relative movement of α and β subunits	(95)
KCNQ1 (Kv7.1) K^+ channel	TM segments S1 and S4	S1 and S4 interact differently in open and closed channels	(78)
KCNQ1 (Kv7.1)/KCNE1 K^+ channel complex	Disulfides between KCNQ1 and KCNE1	Relative movement of two subunits involved in channel gating	(72, 96, 97)
hERG K^+ channel	Intracellular N-terminus and S4-S5 linker	Two parts of protein interact in closed channels	(98)
Na^+ channel	Outer pore	Outer pore movement involved in channel slow inactivation	(99)
Na^+ channel	TM segments S2 and S4	Interact during voltage-dependent activation	(100, 101)
Cyclic nucleotide gated channel	Cytoplasmic C-terminus	Close inter-subunit proximity in open channels	(102)
Cyclic nucleotide gated channel	TM segments S5 and S6	Opening and closing involves rotational movement of TMs	(103)
HCN channel	TM segments S4 and S5	Membrane depolarization causes extracellular ends of TMs to move together	(104)
Ligand-gated channels			
$GABA_A$ receptor	TM α-helices	Channel opening and closing involves inter- and intra-subunit relative movements of different TMs	(105–109)
Glutamate receptors	Extracellular LBD	Movement of LBD triggers channel opening	(110–113)
Glutamate receptors	Extracellular linkers between TMs and LBD	Linker movement required for channel opening	(114, 115)
P2X ATP receptor	Extracellular domain	Conformational changes required for channel opening	(116, 117)
P2X ATP receptor	Outer vestibule of channel pore	Outer vestibule does not have to dilate for pore to open	(118)
P2X ATP receptor	TM α-helices	Channel opening requires intra-subunit TM movement	(119)
Glycine receptor	TM α-helices and extracellular loops	Relative movement of TMs and loops during channel opening	(120, 121)
Other channel types			
ASIC (acid-sensitive channels)	Extracellular loops	Close apposition of two loops occurs during receptor desensitization	(122)
ASIC (acid-sensitive channels)	Outer pore	Channel opening involves rotation of different TMs	(123)
CFTR Cl^- channel	Outer pore	Channel opening involves relative lateral movement of different TMs	(88)
CFTR Cl^- channel	Extracellular loops	Loops move relative to each other during channel opening	(124)

Selected examples of studies using electrophysiological techniques to investigate the effects of disulfide bond formation on the function of different ion channel types – categorized into voltage-gated channel superfamily, ligand-gated channels, and other channel types – illustrating the range of different conformational information that can potentially be obtained using such an approach. Disulfide bond formation was either spontaneous or resulted from exposure to oxidant such as CuPhe, H_2O_2, or I_2. Disulfide bonds (spontaneous or induced) could be broken by exposure to reducing agent such as DTT. Formation and/or breakage of disulfide bonds led to some change in channel function as determined by electrophysiological investigation of channel current.

which the side-chains in question are retained in the proximal, high-metal-affinity position. Zinc bridges between introduced histidine side-chains have also been used in the study of some ion channels (see Table 2). Because metal binding is reversible, and its affinity is strongly dependent on protein conformation (*via* conformation-dependent changes in the proximity of amino acid side-chains), this metal bridge approach is considered more likely to reflect normal, natural protein conformations and to be far less sensitive to the effects of rare protein conformations in which amino acid side-chains briefly come into close proximity. Furthermore, reversible metal binding means that protein conformational changes can continue to occur as the metal ion binds and unbinds from the introduced binding site. In effect, metal bridges act to stabilize natural protein conformations rather than to freeze the protein in a conformation that may or may not occur during normal activity.

In most cases, Cd^{2+} bridges between introduced cysteine side-chains are used to identify pairs of amino acids that are located in close proximity (see Table 2). To ensure that the Cd^{2+} bridge is formed between the introduced cysteine side-chains, use of a cys-less protein background is strongly advisable (see above). Cadmium ions also bind to other amino acid side-chains (histidine, aspartate, glutamate), and so it is possible that Cd^{2+} bridges may form between an introduced cysteine and a nearby non-cysteine side-chain (74–76). In electrophysiological recordings, application of Cd^{2+} may, *via* formation of a metal bridge between introduced cysteines, 'lock' or stabilize the channel in the open conformation (suggesting proximity of two or more cysteine side-chains in the open state) (Figure 1E) or in the closed conformation (suggesting proximity of cysteines in the closed state) (74, 77–80). This locking effect allows strict spatial constraints to be placed on the proximity of different protein regions in different conformational states (Figure 1E). For example, in voltage-gated K^+ channels, evidence from metal bridges formed between identified amino acid side-chains has been used to identify the conformational changes that open the gate in the pore (74), the movements of the voltage-sensor domain that result in voltage-dependent activation (78, 81–87), and relative movements of the voltage-sensor and pore domains during channel opening (77, 83) (Table 2). Furthermore, manipulations that alter the proportion of time that the channel spends in the open state may influence the observed affinity of Cd^{2+} binding, by altering the likelihood that two cysteines that show state-dependent changes in proximity spend in a position that is amenable to metal bridge formation. For example, our own work on the CFTR Cl^- channel has shown that a mutation that keeps the channel in a permanently open state strengthens the apparent affinity of Cd^{2+} binding coordinated by certain pairs of cysteines introduced into the channel pore (80, 88), suggesting that these cysteines are close enough to form metal bridges only in the open state. Meanwhile, Cd^{2+} binding was practically abolished in permanently open channels for other cysteine pairs (80, 88), suggesting that metal bridges form here only when the channel is closed and that the cysteines in question move apart when the channel opens. Structural implications of these experimental findings are described in Figure 3.

The binding affinity of Cd^{2+} for cysteines introduced into a protein is expected to be influenced by the number of cysteine side-chains that can coordinate the Cd^{2+} ion. In metalloproteins Cd^{2+} is almost always coordinated by binding to four cysteine side-chains in a tetrahedral coordination geometry (3–6, 89, 90). The Cd^{2+} binding affinity of such well-coordinated tetra-cysteine binding sites is estimated to be on the order of 10^{-14} M (10 fM) (4). Zinc binding to cysteine or histidine side-chains in proteins also usually occurs in a tetrahedral geometry (3, 5, 90). Electrophysiological investigation of ion channels often suggests Cd^{2+} binding to a single cysteine side-chain with a measured affinity of >100 μM (32, 80, 91), whereas measured affinities of <1 μM have been reported with two proximal cysteine side-chains (32, 57, 77, 80, 91). These quantitative reports are consistent with the suggestion that each additional well-positioned, coordinating cysteine ligand increases Cd^{2+} binding affinity by a factor of ~1000-fold (79). However, it is unlikely that two or more cysteine side-chains introduced experimentally into an ion channel could match the exact coordination geometry found in metalloproteins, and so considerably lower apparent affinities of Cd^{2+} binding are not unexpected experimentally. Furthermore, in some cases, it may not be known how many introduced cysteine side-chains can interact simultaneously with a bound Cd^{2+} ion. In the case of monomeric ion channel proteins, the number of introduced cysteines is known, and in these cases, the measured affinity of Cd^{2+} binding with two cysteines can be compared directly with the affinity when only one cysteine is present (32, 57, 80, 91). In the case of multimeric proteins, however, introduction of only a single cysteine into each subunit may result in the formation of inter-subunit metal bridges of unknown coordination geometry. For example, in tetrameric K^+ channels (92, 93) and trimeric P2X receptor channels (40), it has been observed that a single cysteine substitution results in very high affinity Cd^{2+} binding, which has been used to suggest that more than two cysteine side-chains are able to interact simultaneously with the bound Cd^{2+} ion to

Table 2: Examples of conformational changes in ion channels probed by formation of metal bridges.

Channel type	Metal ion	Region of channel protein	Conformational information obtained	References
Voltage-gated channel superfamily				
Voltage-gated Na^+ channel	Cd^{2+}, Zn^{2+} (1–100 μM)	Pore	Movement during opening and closing	(57, 91)
Voltage-gated K^+ channel	Cd^{2+} (0.1–100 μM)	Pore	Movement during opening and closing	(60, 74)
Voltage-gated K^+ channel	Cd^{2+} (0.1–1 μM)	Pore and voltage sensor	Proximity changes during voltage gating	(77)
Voltage-gated K^+ channel	Cd^{2+} (0.1–100 μM)	Voltage sensor	Different kinds of movement during voltage gating	(78, 81, 82, 86, 87)
Voltage-gated K^+ channel	Zn^{2+} (histidine) (1–10 μM)	Voltage sensor		(81, 83–85)
Inward rectifier K^+ channel	Cd^{2+} (10–100 μM)	Pore	Movement during opening and closing	(93, 125)
HCN	Cd^{2+} (0.1–1 μM)	Intracellular C-terminus and S4-S5 linker	Interaction involved in channel gating	(79, 126)
Ligand-gated channels				
Glutamate receptor	Cd^{2+} (10–100 μM)	Pore	Widespread movement during opening and closing	(127)
5-HT_3 receptor	Cd^{2+} (1–200 μM)	Pore	Minor pore rearrangement during opening and closing	(128)
P2X ATP receptor	Cd^{2+} (0.4–20 μM)	Pore	Movement during opening and closing	(41, 75, 129)
P2X ATP receptor	Cd^{2+} (30–300 μM)	Extracellular linker	Moves during opening and closing	(130)
Other channel types				
Connexins	Cd^{2+} (0.1–60 μM)	Pore	Movement during opening and closing	(131, 132)
CFTR Cl^- channel	Cd^{2+} (1–10 μM)	Outer pore	Translational movement during opening and closing	(88)
CFTR Cl^- channel	Cd^{2+} (0.1–10 μM)	Outer pore	Lateral movement during opening and closing	(80)

Selected examples of studies using electrophysiological techniques to investigate the effects of metal bridge formation on the function of different ion channel types – categorized into voltage-gated channel superfamily, ligand-gated channels, and other channel types – illustrating the range of different conformational information that can potentially be obtained using such an approach. Metal bridges were formed by application of Cd^{2+} or Zn^{2+} (as indicated) and coordinated by introduced cysteine side-chains (or histidine side-chains where indicated). The approximate concentration range of Cd^{2+} or Zn^{2+} that was required to cause changes in channel function that were taken as evidence for the formation of metal bridges is indicated in parentheses. Formation of metal bridges led to some change in channel function as determined by electrophysiological investigation of channel current.

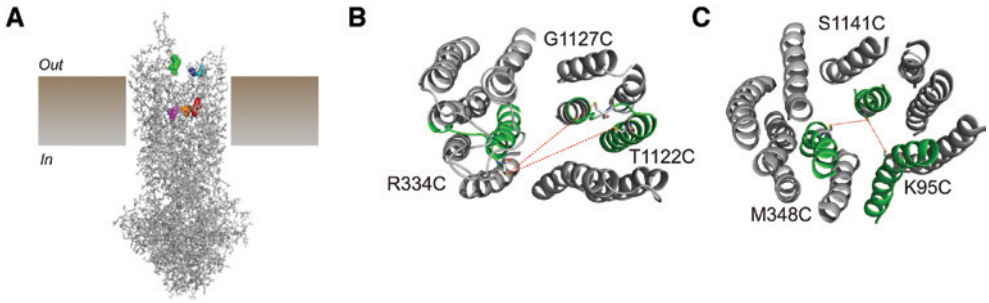

Figure 3: Examples of the use of metal bridges to determine conformation-dependent distances in the CFTR Cl^- channel pore. (A) Overall atomic homology structure of the CFTR protein within the cell membrane, according to coordinates provided by Mornon et al. (133). The location of pore-lining amino acids that have been studied in our laboratory using cysteine mutagenesis and Cd^{2+} bridge formation are indicated, close to the outer mouth of the pore (R334, green; T1122, cyan; G1127, blue), and the inner vestibule of the pore (K95, red; M348, purple; S1141, orange). (B, C) Location of identified introduced cysteine side-chains that could form conformation-dependent Cd^{2+} bridges at these levels of the pore, viewed from the extracellular side of the membrane. (B) R334C was reported to form a Cd^{2+} bridge with T1122C in open channels and with G1127C in closed channels (88). The measured S-S distances (red dotted lines) are 22.2 Å for R334C-T1122C and 21.1 Å for R334C-G1127C, inconsistent with metal bridge formation, which suggests that this model does not accurately represent the geometry of this part of either the open or the closed channel. (C) S1141C was reported to form a Cd^{2+} bridge with K95C in open channels and with M348C in closed channels (80). The measured S-S distances (red dotted lines) are 8.6 Å for K95C-S1141C and 8.2 Å for M348C-S1141C, close to distances required for Cd^{2+} coordination, suggesting that only small conformational changes at this level of the pore may occur during pore opening and closing.

form a high-affinity Cd^{2+} binding site. Besides the number of interacting cysteine side-chains, other factors may influence the apparent affinity of Cd^{2+} binding measured in electrophysiological experiments, including ease of access of the Cd^{2+} ion from the bulk solution on one side of the membrane to its binding site, the exact proximity and relative orientation of introduced cysteine side-chains, local structural features such as the presence of other potentially interacting side-chains such as histidines, aspartates, and glutamates, conformational changes and dynamic protein flexibility that influence the proportion of the time that cysteine side-chains are in a permissive position for Cd^{2+} bridge formation, strain on the metal bridge due to sub-optimal coordination, and the propensity of the channel to undergo conformational changes that can break conformationally sensitive Cd^{2+} bridges. As illustrated in Table 2, the range of Cd^{2+} concentrations that have been used experimentally to provide evidence for metal bridge formation between introduced cysteine side-chains in ion channel proteins span several orders of magnitude.

As with disulfide bond formation, identification of metal bridges is used to suggest strict spatial constraints on the structure of channel proteins. Structural studies with a number of model systems suggest a Cd^{2+}-S distance of ~2.5 Å (3, 6, 89, 90), implying an S-S distance between coordinating cysteine side-chains of ~5 Å (Figure 2). The Zn^{2+}-S distance for binding to cysteine is similar, ~2.3 Å, while the Zn^{2+}-N distance for binding to histidine is reportedly ~2.1 Å (3, 90).

Conclusions

Techniques that take advantage of the reactivity of introduced cysteine side-chains have been used to probe the structure and function of practically all known types of ion channels; the examples cited in Tables 1 and 2 represent just a small representative sample of the kinds of important dynamic rearrangements that have been identified in different channel types. Metal bridges positively identified as being formed between different regions of ion channel proteins can give invaluable structural constraints that are otherwise inaccessible in the study of these integral membrane proteins, while at the same time allowing normal conformational rearrangements to proceed. These functional techniques therefore provide a powerful complement and constraint to structural techniques such as X-ray crystallography.

List of abbreviations

β-ME	β-mercaptoethanol
CFTR	cystic fibrosis transmembrane conductance regulator
CuPhe	copper(II)-*o*-phenanthroline
DTT	dithiothreitol
LBD	ligand binding domain
MTS	methanethiosulfonate
MTSEA	[2-aminoethyl] methanethiosulfonate
MTSES	[2-sulfonatoethyl] methanethiosulfonate
MTSET	[2-(trimethylammonium)ethyl] methanethiosulfonate
SCAM	substituted cysteine accessibility mutagenesis
TM	transmembrane segment

Acknowledgments: Work in the author's laboratory concerning conformational changes in the CFTR Cl^- channel is funded by the Canadian Institutes of Health Research and Cystic Fibrosis Canada.

References

1. Sevier CS, Kaiser CA. Formation and transfer of disulphide bonds in living cells. Nat Rev Mol Cell Biol 2002; 3: 836–47.
2. Cremers CM, Jakob U. Oxidant sensing by reversible disulfide bond formation. J Biol Chem 2013; 288: 26489–96.
3. Rulíšek L, Vondrášek J. Coordination geometries of selected transition metal ions (Co^{2+}, Ni^{2+}, Cu^{2+}, Zn^{2+}, Cd^{2+}, and Hg^{2+}) in metalloproteins. J Inorg Biochem 1998; 71: 115–27.
4. Jalilehvand F, Mah V, Leung BO, Mink J, Bernard GM, Hajba L. Cadmium(II) cysteine complexes in the solid state: a multispectroscopic study. Inorg Chem 2009; 48: 4219–30.
5. Freisinger E, Vašák M. Cadmium in metallothioneins. Met Ions Life Sci 2013; 11: 339–71.
6. Dudev T, Lim C. Competition among metal ions for protein binding sites: determinants of metal ion selectivity in proteins. Chem Rev 2014; 114: 538–56.
7. Leung BO, Jalilehvand F, Mah V, Parvez M, Wu Q. Silver(I) complex formation with cysteine, penicillamine, and glutathione. Inorg Chem 2013; 52: 4594–602.
8. Frillingos S, Sahin-Tóth M, Wu J, Kaback HR. Cys-scanning mutagenesis: a novel approach to structure function relationships in polytopic membrane proteins. FASEB J 1998; 12: 1281–99.
9. Loo TW, Clarke DM. Determining the structure and mechanism of the human multidrug resistance P-glycoprotein using cysteine-scanning mutagenesis and thiol-modification techniques. Biochim Biophys Acta 1999; 1461: 315–25.
10. Liapakis G, Simpson MM, Javitch JA. The substituted-cysteine accessibility method (SCAM) to elucidate membrane protein structure. Curr Protoc Neurosci 2001; 4: 4–15.
11. Bass RB, Butler SL, Chervitz SA, Gloor SL, Falke JJ. Use of site-directed cysteine and disulfide chemistry to probe protein structure and dynamics: applications to soluble and transmembrane receptors of bacterial chemotaxis. Methods Enzymol 2007; 423: 25–51.
12. Zhu Q, Casey JR. Topology of transmembrane proteins by scanning cysteine accessibility mutagenesis methodology. Methods 2007; 41: 439–50.
13. Takeuchi A, Reyes N, Artigas P, Gadsby DC. Visualizing the mapped ion pathway through the Na,K-ATPase pump. Channels 2009; 3: 383–6.
14. Terada T, Inui K. Recent advances in structural biology of peptide transporters. Curr Top Membr 2012; 70: 257–74.
15. Hilwi M, Dayan O, Kanner BI. Conformationally sensitive proximity of extracellular loops 2 and 4 of the γ-aminobutyric acid (GABA) transporter GAT-1 inferred from paired cysteine mutagenesis. J Biol Chem 2014; 289: 34258–66.
16. Loo TW, Clarke DM. Cysteines introduced into extracellular loops 1 and 4 of human P-glycoprotein that are close only in the open conformation spontaneously form a disulfide bond that inhibits drug efflux and ATPase activity. J Biol Chem 2014; 289: 24749–58.
17. Monette MY, Somasekharan S, Forbush B. Molecular motions involved in Na-K-Cl cotransporter-mediated ion transport and transporter activation revealed by internal cross-linking between transmembrane domains 10 and 11/12. J Biol Chem 2014; 289: 7569–79.
18. Akabas MH, Stauffer DA, Xu M, Karlin A. Acetylcholine receptor channel structure probed in cysteine-substitution mutants. Science 1992; 258: 307–10.
19. Akabas MH, Kaufmann C, Archdeacon P, Karlin A. Identification of acetylcholine receptor channel-lining residues in the entire M2 segment of the α subunit. Neuron 1994; 13: 919–27.
20. Karlin A, Akabas MH. Substituted-cysteine accessibility method. Methods Enzymol 1998; 293: 123–45.
21. Loo TW, Clarke DM. Using a cysteine-less mutant to provide insight into the structure and mechanism of CFTR. J Physiol 2006; 572: 312.
22. Li M-S, Demsey AFA, Qi J, Linsdell P. Cysteine-independent inhibition of the CFTR chloride channel by the cysteine-reactive reagent sodium (2-sulphonatoethyl) methanethiosulphonate. Br J Pharmacol 2009; 157: 1065–71.
23. Holstead RG, Li M-S, Linsdell P. Functional differences in pore properties between wild-type and cysteine-less forms of the CFTR chloride channel. J Membr Biol 2011; 243: 15–23.
24. El Hiani Y, Linsdell P. Role of the juxtamembrane region of cytoplasmic loop 3 in the gating and conductance of the cystic fibrosis transmembrane conductance regulator chloride channel. Biochemistry 2012; 51: 3971–81.
25. Bai Y, Li M, Hwang T-C. Dual roles of the sixth transmembrane segment of the CFTR chloride channel in gating and permeation. J Gen Physiol 2010; 136: 293–309.
26. El Hiani Y, Linsdell P. Functional architecture of the cytoplasmic entrance to the cystic fibrosis transmembrane conductance regulator chloride channel pore. J Biol Chem 2015; 290: 15855–65.
27. Dudev T, Lim C. Metal binding affinity and selectivity in metalloproteins: insights from computational studies. Annu Rev Biophys 2008; 37: 97–116.
28. Shannon RD. Revised effective ionic radii and systematic studies of interatomic distances in halides and chalcogenides. Acta Cryst 1976; A32: 751–67.
29. Lü Q, Miller C. Silver as a probe of pore-forming residues in a potassium channel. Science 1995; 268: 304–7.
30. Pérez-García MT, Chiamvimonvat N, Marban E, Tomaselli GF. Structure of the sodium channel pore revealed by serial cysteine mutagenesis. Proc Natl Acad Sci USA 1996; 93: 300–4.
31. Webster SM, del Camino D, Dekker JP, Yellen G. Intracellular gate opening in Shaker K^+ channels defined by high-affinity metal bridges. Nature 2004; 428: 864–8.
32. Choi L-S, Mach T, Bayley H. Rates and stoichiometries of metal ion probes of cysteine residues within ion channels. Biophys J 2013; 105: 356–64.
33. del Camino D, Yellen G. Tight steric closure at the intracellular activation gate of a voltage-gated K^+ channel. Neuron 2001; 32: 649–56.
34. Xiao J, Zhen X-g, Yang J. Localization of PIP_2 activation gate in inward rectifier K^+ channels. Nature Neurosci 2003; 6: 811–8.
35. Bruening-Wright A, Lee W-S, Adelman JP, Maylie J. Evidence for a deep pore activation gate in small conductance Ca^{2+}-activated K^+ channels. J Gen Physiol 2007; 130: 601–10.

36. Klein H, Garneau L, Banderali U, Simoes M, Parent L, Sauvé R. Structural determinants of the closed KCa3.1 channel pore in relation to channel gating: results from a substituted cysteine accessibility analysis. J Gen Physiol 2007; 129: 299–315.
37. Rothberg BS, Shin KS, Phale PS, Yellen G. Voltage-controlled gating at the intracellular entrance to a hyperpolarization-activated cation channel. J Gen Physiol 2002; 119: 83–91.
38. Contreras JE, Srikumar D, Holmgren M. Gating at the selectivity filter in cyclic nucleotide-gated channels. Proc Natl Acad Sci USA 2008; 105: 3310–4.
39. Salazar H, Jara-Oseguera A, Hernández-García E, Llorente I, Arias-Olguín II, Soriano-García M, Islas LD, Rosenbaum T. Structural determinants of gating in the TRPV1 channel. Nature Struct Mol Biol 2009; 16: 704–10.
40. Li M, Chang T-H, Silberberg SD, Swartz KJ. Gating the pore of P2X receptor channels. Nat Neurosci 2008; 11: 883–7.
41. Kracun S, Chaptal V, Abramson J, Khakh BS. Gated access to the pore of a P2X receptor. Structural implications for closed-open transitions. J Biol Chem 2010; 285: 10110–21.
42. Yellen G, Sodickson D, Chen T-Y, Jurman ME. An engineered cysteine in the external mouth of a K^+ channel allows inactivation to be modulated by metal binding. Biophys J 1994; 66: 1068–75.
43. Liu Y, Jurman ME, Yellen G. Dynamic rearrangement of the outer mouth of a K^+ channel during gating. Neuron 1996; 16: 859–67.
44. Szendroedi J, Sandtner W, Zarrabi T, Zebedin E, Hilber K, Dudley SC, Fozzard HA, Todt H. Speeding the recovery from ultraslow inactivation of voltage-gated Na^+ channels by metal ion binding to the selectivity filter: a foot-on-the door? Biophys J 2007; 93: 4209–24.
45. Raghuraman H, Cordero-Morales JF, Jogini V, Pan AC, Kollewe A, Roux B, Perozo E. Mechanism of Cd^{2+} coordination during slow inactivation in potassium channels. Structure 2012; 20: 1332–42.
46. Beck EJ, Yang Y, Yaemsiri S, Raghuram V. Conformational changes in a pore-lining helix coupled to cystic fibrosis transmembrane conductance regulator channel gating. J Biol Chem 2008; 283: 4957–66.
47. Serrano JR, Liu X, Borg ER, Alexander CS, Shaw CF, Dawson DC. CFTR: ligand exchange between a permeant anion ($[Au(CN)_2]^-$) and an engineered cysteine (T338C) blocks the pore. Biophys J 2006; 91: 1737–48.
48. Alexander C, Ivetac A, Liu X, Norimatsu Y, Serrano JR, Landstrom A, Sansom M, Dawson DC. Cystic fibrosis transmembrane conductance regulator: using differential reactivity toward channel-permeant and channel-impermeant thiol-reactive probes to test a molecular model for the pore. Biochemistry 2009; 48: 10078–88.
49. Smith SS, Steinle ED, Meyerhoff ME, Dawson DC. Cystic fibrosis transmembrane conductance regulator. Physical basis for lyotropic anion selectivity patterns. J Gen Physiol 1999; 114: 799–818.
50. Gong X, Burbridge SM, Cowley EA, Linsdell P. Molecular determinants of $Au(CN)_2^-$ binding and permeability within the cystic fibrosis transmembrane conductance regulator Cl^- channel pore. J Physiol 2002; 540: 39–47.
51. Fatehi M, Linsdell P. State-dependent access of anions to the cystic fibrosis transmembrane conductance regulator chloride channel pore. J Biol Chem 2008; 283: 6102–9.
52. Norimatsu Y, Ivetac A, Alexander C, Kirkham J, O'Donnell N, Dawson DC, Sansom MSP. Cystic fibrosis transmembrane conductance regulator: a molecular model defines the architecture of the anion conduction path and locates a "bottleneck" in the pore. Biochemistry 2012; 51: 2199–212.
53. Wang W, Linsdell P. Conformational change opening the CFTR chloride channel pore coupled to ATP-dependent gating. Biochim Biophys Acta 2012; 1818: 851–60.
54. Wang W, Linsdell P. Alternating access to the transmembrane domain of the ATP-binding cassette protein cystic fibrosis transmembrane conductance regulator (ABCC7). J Biol Chem 2012; 287: 10156–65.
55. Gao X, Hwang T-C. Localizing a gate in CFTR. Proc Natl Acad Sci USA 2015; 112: 2461–6.
56. El Hiani Y, Linsdell P. Changes in accessibility of cytoplasmic substances to the pore associated with activation of the cystic fibrosis transmembrane conductance regulator chloride channel. J Biol Chem 2010; 285: 32126–40.
57. Bénitah J-P, Tomaselli GF, Marban E. Adjacent pore-lining residues within sodium channels identified by paired cysteine mutagenesis. Proc Natl Acad Sci USA 1996; 93: 7392–6.
58. Zhang H-J, Liu Y, Zühlke RD, Joho RH. Oxidation of an engineered pore cysteine locks a voltage-gated K^+ channel in a nonconducting state. Biophys J 1996; 71: 3083–90.
59. Gordon SE, Varnum MD, Zagotta WN. Direct interaction between amino- and carboxyl-terminal domains of cyclic nucleotide-gated channels. Neuron 1997; 19: 431–41.
60. Krovetz HS, VanDongen HM, VanDongen AM. Atomic distance estimates from disulfides and high-affinity metal-binding sites in a K^+ channel pore. Biophys J 1997; 72: 117–26.
61. Kobashi K. Catalytic oxidation of sulfhydryl groups by o-phenanthroline copper complex. Biochim Biophys Acta 1968; 158: 239–45.
62. Careaga CL, Falke JJ. Structure and dynamics of Escherichia coli chemosensory receptors. Engineered sulfhydryl studies. Biophys J 1992; 62: 209–19.
63. Careaga CL, Falke JJ. Thermal motions of surface α-helices in the D-galactose chemosensory receptor: detection by disulfide trapping. J Mol Biol 1992; 226: 1219–35.
64. Sowdhamini R, Srinivasan N, Shoichet B, Santi DV, Ramakrishnan C, Balaram P. Stereochemical modeling of disulfide bridges. Criteria for introduction into proteins by site-directed mutagenesis. Prot Eng 1989; 3: 95–103.
65. Srinivasan N, Sowdhamini R, Ramakrishnan C, Balaram P. Conformations of disulfide bridges in proteins. Int J Pept Protein Res 1990; 36: 147–55.
66. Schmidt B, Ho L, Hogg PJ. Allosteric disulfide bonds. Biochemistry 2006; 45: 7429–33.
67. Loo TW, Clarke DM. Determining the dimensions of the drug-binding domain of human P-glycoprotein using thiol cross-linking compounds as molecular rulers. J Biol Chem 2001; 276: 36877–80.
68. Chen EY, Bartlett MC, Loo TW, Clarke DM. The deltaF508 mutation disrupts packing of the transmembrane segments of the cystic fibrosis transmembrane conductance regulator. J Biol Chem 2004; 279: 39620–7.
69. Wang Y, Loo TW, Bartlett MC, Clarke DM. Correctors promote maturation of cystic fibrosis transmembrane conductance regulator (CFTR)-processing mutants by binding to the protein. J Biol Chem 2007; 282: 33247–51.

70. Zhou Y, Guan L, Freites JA, Kaback HR. Opening and closing of the periplasmic gate in lactose permease. Proc Natl Acad Sci USA 2008; 105: 3774–8.
71. Nair AV, Nguyen CH, Mazzolini M. Conformational rearrangements in the S6 domain and C-linker during gating in CNGA1 channels. Eur Biophys J 2009; 38: 993–1002.
72. Wang YH, Jiang M, Xu XL, Hsu K-L, Zhang M, Tseng G-N. Gating-related molecular motions in the extracellular domain of the I_{Ks} channel: implications for I_{Ks} channelopathy. J Membr Biol 2011; 239: 137–56.
73. Collier DM, Tomkovicz VR, Peterson ZJ, Benson CJ, Snyder PM. Intersubunit conformational changes mediate epithelial sodium channel gating. J Gen Physiol 2014; 144: 337–48.
74. Holmgren M, Shin KS, Yellen G. The activation gate of a voltage-gated K^+ channel can be trapped in the open state by an intersubunit metal bridge. Neuron 1998; 21: 617–21.
75. Heymann G, Dai J, Li M, Silberberg SD, Zhou H-X, Swartz KJ. Inter- and intrasubunit interactions between transmembrane helices in the open state of P2X receptor channels. Proc Natl Acad Sci USA 2013; 110: E4045–54.
76. Zhou Y, Xia X-M, Lingle CJ. Cadmium-cysteine coordination in the BK inner pore region and its structural and functional implications. Proc Natl Acad Sci USA 2015; 112: 5237–42.
77. Neale EJ, Elliott DJS, Hunter M, Sivaprasadarao A. Evidence for intersubunit interactions between S4 and S5 transmembrane segments of the Shaker potassium channel. J Biol Chem 2003; 278: 29079–85.
78. Haitin Y, Yisharel I, Malka E, Shamgar L, Schottelndreier H, Peretz A, Paas Y, Attali B. S1 constrains S4 in the voltage sensor domain of Kv7.1 K^+ channels. PLoS One 2008; 3: e1935.
79. Kwan DCH, Prole DL, Yellen G. Structural changes during HCN channel gating defined by high affinity metal bridges. J Gen Physiol 2012; 140: 279–91.
80. El Hiani Y, Linsdell P. Metal bridges illuminate transmembrane domain movements during gating of the cystic fibrosis transmembrane conductance regulator chloride channel. J Biol Chem 2014; 289: 28149–59.
81. Lainé M, Lin M-cA, Bannister JPA, Silverman WR, Mock AF, Roux B, Papazian DM. Atomic proximity between S4 segments and pore domain in Shaker potassium channels. Neuron 2003; 39: 467–81.
82. Campos FV, Chanda B, Roux B, Bezanilla F. Two atomic constraints unambiguously position the S4 segment relative to S1 and S2 segments in the closed state of Shaker K channel. Proc Natl Acad Sci USA 2007; 104: 7904–9.
83. Lewis A, Jogini V, Blachowicz L, Lainé M, Roux B. Atomic constraints between the voltage sensor and the pore domain in a voltage-gated K^+ channel of known structure. J Gen Physiol 2008; 549–61.
84. Phillips LR, Swartz KJ. Position and motions of the S4 helix during opening of the Shaker potassium channel. J Gen Physiol 2010; 136: 629–44.
85. Lin M-c, Hsieh J-Y, Mock AF, Papazian DM. R1 in the Shaker S4 occupies the gating charge transfer center in the resting state. J Gen Physiol 2011; 138: 155–63.
86. Henrion U, Renhorn J, Börjesson SI, Nelson EM, Schwaiger CS, Bjelkmar P, Wallner B, Lindahl E, Elinder F. Tracking a complete voltage-sensor cycle with metal-ion bridges. Proc Natl Acad Sci USA 2012; 109: 8552–7.
87. Gourgy-Hacohen O, Kornilov P, Pittel I, Peretz A, Attali B, Paas Y. Capturing distinct KCNQ2 channel resting states by metal ion bridges in the voltage-sensor domain. J Gen Physiol 2014; 144: 513–27.
88. Wang W, Linsdell P. Relative movements of transmembrane regions at the outer mouth of the cystic fibrosis transmembrane conductance regulator channel pore during channel gating. J Biol Chem 2012; 287: 32136–46.
89. Enescu M, Renault J-P, Pommeret S, Mialocq J-C, Pin S. Ab initio study of Cd-thiol complexes: application to the modelling of the metallothionein active site. Phys Chem Chem Phys 2003; 5: 3762–7.
90. Dokmanić I, Šikić M, Tomić S. Metals in proteins: correlation between the metal-ion type, coordination number and the amino-acid residues involved in the coordination. Acta Crys 2008; D64: 257–63.
91. Tsushima RG, Li RA, Backx PH. P-loop flexibility in Na^+ channel pores revealed by single-and double-cysteine replacements. J Gen Physiol 1997; 110: 59–72.
92. Liu Y, Holmgren M, Jurman ME, Yellen G. Gated access to the pore of a voltage-dependent K^+ channel. Neuron 1997; 19: 175–84.
93. Loussouarn G, Makhina EN, Rose T, Nichols CG. Structure and dynamics of the pore of inwardly rectifying K_{ATP} channels. J Biol Chem 2000; 275: 1137–44.
94. Liu G, Zakharov SI, Yang L, Deng S-X, Landry DW, Karlin A, Marx SO. Position and role of the BK channel α subunit S0 helix inferred from disulfide crosslinking. J Gen Physiol 2008; 131: 537–48.
95. Liu G, Zakharov SI, Yang L, Wu RS, Deng S-X, Landry DW, Karlin A, Marx SO. Locations of the β1 transmembrane helices in the BK potassium channel. Proc Natl Acad Sci USA 2008; 105: 10727–32.
96. Chung DY, Chan PJ, Bankston JR, Yang L, Liu G, Marx SO, Karlin A, Kass RS. Location of KCNE1 relative to KCNQ1 in the I_{KS} potassium channel by disulfide cross-linking of substituted cysteines. Proc Natl Acad Sci USA 2009; 106: 743–8.
97. Lvov A, Gage SD, Berrios VM, Kobertz WR. Identification of a protein-protein interaction between KCNE1 and the activation gate machinery of KCNQ1. J Gen Physiol 2009; 135: 607–18.
98. de la Peña P, Alonso-Ron C, Machin A, Fernández-Trillo J, Carretero L, Domínguez P, Barros F. Demonstration of physical proximity between the N terminus and the S4-S5 linker of the human ether-à-go-go-related gene (hERG) potassium channel. J Biol Chem 2011; 286: 19065–75.
99. Xiong W, Li RA, Tian Y, Tomaselli GF. Molecular motions of the outer ring of charge of the sodium channel: do they couple to slow inactivation? J Gen Physiol 2003; 122: 323–32.
100. DeCaen PG, Yarov-Yarovoy V, Zhao Y, Scheuer T, Catterall WA. Disulfide locking a sodium channel voltage sensor reveals ion pair formation during activation. Proc Natl Acad Sci USA 2008; 105: 15142–7.
101. DeCaen PG, Yarov-Yarovoy V, Sharp EM, Scheuer T, Catterall WA. Sequential formation of ion pairs during activation of a sodium channel voltage sensor. Proc Natl Acad Sci USA 2009; 106: 22498–503.
102. Hua L, Gordon SE. Functional interactions between A′ helices in the C-linker of open CNG channels. J Gen Physiol 2005; 125: 335–44.
103. Nair AV, Mazzolini M, Codega P, Giorgetti A, Torre V. Locking CNGA1 channels in the open and closed states. Biophys J 2006; 90: 3599–607.

104. Bell DC, Turbendian HK, Valley MT, Zhou L, Riley JH, Siegelbaum SA, Tibbs GR. Probing S4 and S5 segment proximity in mammalian hyperpolarization-activated HCN channels by disulfide bridging and Cd^{2+} coordination. Pflügers Arch 2009; 458: 259–72.
105. Horenstein J, Wagner DA, Czajkowsky C, Akabas MH. Protein mobility and GABA-induced conformational changes in $GABA_A$ receptor pore-lining M2 segment. Nat Neurosci 2001; 4: 477–85.
106. Jansen M, Akabas MH. State-dependent cross-linking of the M2 and M3 segments: functional basis for the alignment of $GABA_A$ and acetylcholine receptor M3 segments. J Neurosci 2006; 26: 4492–9.
107. Yang Z, Webb TI, Lynch JW. Closed-state cross-linking of adjacent β1 subunits in α1β1 $GABA_a$ receptors via introduced 6′ cysteines. J Biol Chem 2007; 282: 16803–10.
108. Bali M, Jansen M, Akabas MH. GABA-induced intersubunit conformational movement in the $GABA_A$ receptor α1M1-β2M3 transmembrane subunit interface: experimental basis for homology modeling of an intravenous anesthetic binding site. J Neurosci 2009; 29: 3083–92.
109. Bali M, Akabas MH. Gating-induced conformational rearrangement of the γ-aminobutyric acid type A receptor β-α subunit interface in the membrane-spanning domain. J Biol Chem 2012; 287: 27762–70.
110. Blanke ML, Vandongen AM. Constitutive activation of the N-methyl-D-aspartate receptor via cleft-spanning disulfide bonds. J Biol Chem 2008; 283: 21519–29.
111. Ahmed AH, Wang S, Chuang H-H, Oswald RE. Mechanism of AMPA receptor activation by partial agonists. Disulfide trapping of closed lobe conformations. J Biol Chem 2011; 286: 35257–66.
112. Daniels BA, Andrews ED, Aurousseau MRP, Accardi MV, Bowie D. Crosslinking the ligand-binding domain dimer interface locks kainate receptors out of the main open state. J Physiol 2013; 591: 3873–85.
113. Yelshanskaya MV, Li M, Sobolevsky AI. Structure of an agonist-bound ionotropic glutamate receptor. Science 2014; 345: 1070–4.
114. Talukder I, Wollmuth LP. Local constraints in either the GluN1 or GluN2 subunit equally impair NMDA receptor pore opening. J Gen Physiol 2011; 138: 179–94.
115. Kazi R, Gan Q, Talukder I, Markowitz M, Salussolia CL, Wollmuth LP. Asynchronous movements prior to pore opening in NMDA receptors. J Neurosci 2013; 33: 12052–66.
116. Roberts JA, Allsopp RC, El Ajouz S, Vial C, Schmid R, Young MT, Evans RJ. Agonist binding evokes extensive conformational changes in the extracellular domain of the ATP-gated P2X1 receptor ion channel. Proc Natl Acad Sci USA 2012; 109: 4663–7.
117. Stelmashenko O, Compan V, Browne LE, North RA. Ectodomain movements of an ATP-gated ion channel (P2X2 receptor) probed by disulfide locking. J Biol Chem 2014; 289: 9909–17.
118. Kawate T, Robertson JL, Li M, Silberberg SD, Swartz KJ. Ion access pathway to the transmembrane pore in P2X receptor channels. J Gen Physiol 2011; 137: 579–90.
119. Liang X, Xu H, Li C, Yin S, Xu T, Liu J, Li Z. Functional identification of close proximity amino acid side chains within the transmembrane-spanning helixes of the P2X2 receptor. PLoS One 2013; 8: e70629.
120. Lobo IA, Harris RA, Trudell JR. Cross-linking of sites involved with alcohol action between transmembrane segments 1 and 3 of the glycine receptor following activation. J Neurochem 2008; 104: 1649–62.
121. Prevost MS, Moraga-Cid G, Van Renterghem C, Edelstein SJ, Changeux J-P, Corringer P-J. Intermediate closed state for glycine receptor function revealed by cysteine cross-linking. Proc Natl Acad Sci USA 2013; 110: 17113–8.
122. Springauf A, Bresenitz P, Gründer S. The interaction between two extracellular linker regions controls sustained opening of acid-sensing ion channel 1. J Biol Chem 2011; 286: 24374–84.
123. Tolino LA, Okumura S, Kashlan OB, Carattino MD. Insights into the mechanism of pore opening of acid-sensing ion channel 1A. J Biol Chem 2011; 286: 16297–307.
124. Broadbent SD, Wang W, Linsdell P. Interaction between 2 extracellular loops influences the activity of the cystic fibrosis transmembrane conductance regulator chloride channel. Biochem Cell Biol 2014; 92: 390–6.
125. Wang S, Alimi Y, Tong A, Nichols CG, Enkvetchakul D. Differential roles of blocking ions in KirBac1.1 tetramer stability. J Biol Chem 2009; 284: 2854–60.
126. Prole DL, Yellen G. Reversal of HCN channel voltage dependence via bridging of the S4-S5 linker and post-S6. J Gen Physiol 2006; 128: 273–82.
127. Sobolevsky AI, Yelshansky MV, Wollmuth LP. The outer pore of the glutamate receptor channel has 2-fold rotational symmetry. Neuron 2004; 41: 367–78.
128. Panicker S, Cruz H, Arrabit C, Suen KF, Slesinger PA. Minimal structural rearrangement of the cytoplasmic pore during activation of the $5\text{-}HT_{3A}$ receptor. J Biol Chem 2004; 279: 28149–58.
129. Li M, Kawate T, Silberberg SD, Swartz KJ. Pore-opening mechanism in trimeric P2X receptor channels. Nat Commun 2010; 1: 44.
130. Keceli B, Kubo Y. Voltage- and ATP-dependent structural rearrangements of the P2X2 receptor associated with gating of the pore. J Physiol 2014; 592: 4657–76.
131. Verselis VK, Trelles MP, Rubinos C, Bargiello TA, Srinivas M. Loop gating of connexin hemichannels involves movement of pore-lining residues in the first extracellular loop domain. J Biol Chem 2009; 284: 4484–93.
132. Kwon T, Tang Q, Bargiello TA. Voltage-dependent gating of the Cx32*43E1 hemichannel: conformational changes at the channel entrances. J Gen Physiol 2013; 141: 243–59.
133. Mornon J-P, Hoffmann B, Jonic S, Lehn P, Callebaut I. Full-open and closed CFTR channels, with lateral tunnels from the cytoplasm and an alternative position of the F508 region, as revealed by molecular dynamics. Cell Mol Life Sci 2015; 72: 1377–403.